



Deep optic nerve head morphology and glaucoma progression in eyes with and without laminar dot sign: a longitudinal comparative study

Eunoo Bak^{1,2} · Won June Lee³ · Jin-Soo Kim^{1,2}  · Jinho Lee^{1,2}  · Ahnul Ha^{1,2} · Yong Woo Kim^{1,2}  · Michael J. A. Girard^{4,5} · Jean Martial Mari⁶ · Jin Wook Jeoung^{1,2}  · Young Kook Kim^{1,2} · Ki Ho Park^{1,2} 

Received: 16 August 2019 / Revised: 15 April 2020 / Accepted: 21 May 2020 / Published online: 4 June 2020

© The Author(s), under exclusive licence to The Royal College of Ophthalmologists 2020

Abstract

Purpose To investigate the association between the laminar dot sign (LDS) and the deep optic nerve head (ONH) structure in eyes with primary-open-angle glaucoma (POAG).

Methods Eighty-four eyes of 84 patients with POAG were prospectively included. All of the patients underwent stereo optic disc photography (SDP), red-free retinal nerve fibre layer (RNFL) photography, SS-OCT, and standard automated perimetry. By evaluating the SDP, patients were classified into laminar dot sign (LDS) and non-LDS groups. The deep structure of the ONH including the anterior prelaminar depth (APLD) and prelaminar tissue thickness (PTT) were quantitated using SS-OCT. Progression was assessed by structural or functional deterioration during the average 4.3 ± 1.2 years of follow-up.

Results The LDS group had deeper APLD (405.47 ± 107.55 vs. 302.45 ± 149.51 , $P < 0.001$) and thinner PTT (74.34 ± 24.46 vs. 137.29 ± 40.07 , $P = 0.001$) relative to the non-LDS group. By multivariate analysis, thin PTT was significantly associated with the presence of LDS (odds ratio = 0.939, $P < 0.001$). Structural progression was detected in 45 eyes (84.9%) in the LDS group and 8 eyes (25.8%) in the non-LDS group. Functional progression was demonstrated in 29 eyes (34.5%) in the LDS group and 6 eyes (19.4%) in the non-LDS group. The eyes with LDS had a significantly higher risk of glaucoma progression ($\chi^2 = 5.00$, degree of freedom = 1, $P = 0.033$).

Conclusions In eyes with POAG, the presence of LDS was associated with thinner prelaminar tissue and faster disease progression.

These authors contributed equally: Young Kook Kim, Ki Ho Park

Supplementary information The online version of this article (<https://doi.org/10.1038/s41433-020-1001-2>) contains supplementary material, which is available to authorized users.

✉ Young Kook Kim
md092@naver.com

✉ Ki Ho Park
kihopark@snu.ac.kr

¹ Department of Ophthalmology, Seoul National University College of Medicine, Seoul, Republic of Korea

² Department of Ophthalmology, Seoul National University Hospital, Seoul, Republic of Korea

Introduction

Glaucoma is a progressive optic neuropathy characterised by the degeneration of retinal ganglion cells (RGCs) and their axons. The lamina cribrosa (LC), a complex meshwork of collagenous fibres where RGC axons exit the eye, is considered the main site of RGC injury. The anterior portion of the LC is the prelaminar region, which is

³ Department of Ophthalmology, Hanyang University College of Medicine, Seoul, Republic of Korea

⁴ Department of Biomedical Engineering, National University of Singapore, Singapore, Singapore

⁵ Singapore Eye Research Institute, Singapore National Eye Centre, Singapore, Singapore

⁶ University of French Polynesia, Tahiti, French Polynesia

composed of bundles of RGC axons, astrocytes, capillaries, and extracellular material [1, 2] Prelaminar tissue thickness decreases with glaucoma progression [3, 4], which decrease is known to be associated with mechanical intraocular pressure (IOP) rise [5–8] and vascular dysregulation [9, 10], the main factors contributing to normal-tension glaucoma (NTG)-related glaucomatous optic neuropathy.

Over the past decade, optical coherence tomography (OCT), a non-invasive *in vivo* imaging modality, has been used to view the optic nerve head (ONH) including the LC [11–14]. Swept-source OCT (SS-OCT), using a longer wavelength (1050 nm) than does conventional spectral-domain OCT (SD-OCT), has better tissue penetration and provides higher resolution imaging of the ONH. Recently, widely used OCT findings on the LC have had positive impacts on the diagnosis and management of glaucoma. However, OCT is not available for every clinician, and, recent studies comparing imaging techniques such as SD-OCT, SS-OCT, and others with subjective assessment did not demonstrate any superiority of the former over the latter [15, 16].

One classical ONH sign of glaucoma in inspections of the LC area is the lamellar dot sign (LDS) [17]. This is the representation, by colour-disc photography, of visible grey pores or fenestrae that develop by the loss of neural tissue and deep optic disc cupping, exposing the underlying LC tissue. LDS has been reported to be seen in 29.3% of normal individuals and 70.8% of open-angle glaucoma patients, and is associated with larger vertical cup-to-disc ratio (CDR) and optic disc diameter [18]. However, to the best of our knowledge, there has been no study comparing eyes with and without LDS with OCT and the prospective association with glaucoma progression. Thus, in the present study, we investigated the structure of the ONH in glaucomatous eyes with and without LDS by SD-OCT and SS-OCT and prospectively reviewed the relationship with glaucoma progression.

Materials and methods

This was a prospective longitudinal study designed to evaluate the structure and visual function of glaucoma based on the Swept-Source Optical Coherence Tomography Study of Lamina Cribrosa (SOS-LC), an ongoing prospective study at Seoul National University Hospital. Participants were longitudinally evaluated by a regular follow-up visit protocol, undergoing clinical examination as well as imaging and functional tests. This study's protocol was approved by the Institutional Review Board of Seoul National University Hospital, and its conduct adhered to the tenets of the Declaration of Helsinki.

Participants

For this study, a total of 84 eyes of 84 primary-open-angle glaucoma (POAG) patients at an early stage were enrolled. All of the participants visited the Glaucoma Clinic of Seoul National University Hospital from March 2013 through October 2016.

The inclusion criteria were as follows: (1) POAG with mean deviation (MD) ≥ -6 dB in the visual-field (VF) results; (2) normal-range IOP (≤ 21 mmHg at baseline and during follow-up); (3) an image quality score of 50 or better for all SS-OCT images, and a signal strength of 7 or better for all SD-OCT images.

We defined POAG as the presence of glaucomatous optic disc changes with corresponding glaucomatous VF defects and an open angle confirmed by gonioscopic examination. Glaucomatous optic disc changes were defined as neuroretinal rim thinning, notching, excavation, or RNFL defect. Eyes with glaucomatous VF defects were defined as those with a cluster of three points with probabilities of $<5\%$ on the pattern deviation map in at least 1 hemifield, including at least 1 point with a probability of $<1\%$; or a cluster of two points with a probability of $<1\%$ and a glaucoma hemifield test result outside 99% of age-specific normal limits, or a PSD outside 95% of normal limits. The VF defects were confirmed on two consecutive reliable tests (fixation loss rate $\leq 20\%$, false-positive and false-negative error rates $\leq 25\%$).

The exclusion criteria were as follows: (1) best-corrected visual acuity of $<20/40$; (2) high myopia of spherical equivalence (SE) < -6.0 dioptres (D); (3) history of surgery in the study eye; (4) any other ocular disease or any media opacity that would significantly interfere with OCT image acquisition; (5) lack of sufficiently high-quality images. For cases in which both eyes met all of the eligibility criteria, one eye was randomly chosen as the study eye.

The patients underwent complete ophthalmologic examinations at baseline, including visual acuity testing, slit-lamp examinations, IOP measurements using Goldmann applanation tonometry, stereo optic disc photography (SDP), red-free retinal nerve fibre layer (RNFL) photography (TRC-50IX; Topcon Corporation, Tokyo, Japan), SD-OCT (Cirrus HD-OCT, Carl Zeiss Meditec, Inc., Dublin, CA), SS-OCT (DRI-OCT-1 Atlantis, Topcon, Tokyo, Japan), and standard automated perimetry (SAP) 24-2 testing (Humphrey Field Analyzer; Carl Zeiss Meditec, Dublin, CA, USA). Additionally, the patients attended regular follow-up visits, at which time they underwent clinical examination, disc photography, red-free RNFL photography, SD-OCT, and SAP. Subsequently, all of the patients were administered IOP-lowering treatment. The baseline IOP value was defined as the mean of two measurements before IOP-lowering management was initiated.

The mean IOP was calculated as the average of IOPs throughout the follow-up period.

Presence of LDS

The presence of LDS based on independent evaluation of SDP was determined by two observers (EB and YKK) masked to all other patient information. If the pore or fenestration was visible, the observers graded it as LDS presence, and if not, LDS absence. In cases of disagreement, a third glaucoma specialist (KHP) served as an adjudicator.

OCT

All of the subjects underwent SD-OCT and SS-OCT imaging on the same day, in random order. All of these OCT examinations were performed by one experienced technician. With regard to SD-OCT, the optic disc cube 200×200 protocol was used to measure the ONH and RNFL parameters.

With regard to the SS-OCT meanwhile, to measure the deep optic nerve parameters, five-line cross-scans (five lines horizontal and five lines vertical) centred at the optic disc with 0.25-mm spacing between the cross-lines and 6.0-mm scan width were performed. A total of 32 A-scans were averaged for each line of the five cross lines [19]. The SS-OCT system with its 1050 nm wavelength provided $8 \mu\text{m}$ axial resolution and $20 \mu\text{m}$ lateral resolution at a 100,000 A-scan/s velocity.

Measurement of ONH parameters

To enhance the visibility of the LC configuration on all of the scan images was restored by adaptive enhancement was applied according to previous published protocols [4, 20, 21]. Two experienced ophthalmologists (EB and YKK) who were blinded to all of the patients' clinical information measured all of the parameters using the calliper in the SS-OCT's built-in analysis software (version 9.30). Previous reports indicate that thick retinal vessels can cause large shadows in the OCT cross-sectional scans, thereby preventing visualisation of the structures below. The cross-sectional scan was measured as close as possible to the centre of the ONH, which was identified as the site where the trunk of the central retinal vessels extended from the ONH. The measurements were taken at the closest temporal side of the trunk of the central retinal vessels. On a horizontal scan passing the centre of the disc, we marked a reference line connecting both ends of the Bruch's membrane opening. Three perpendicular lines were marked at the centre and at $100 \mu\text{m}$ nasally and temporally, respectively. The anterior prelaminar depth (APLD) was defined as the distance from the reference line to the anterior

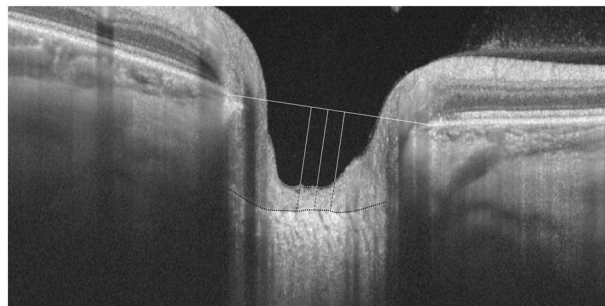


Fig. 1 Swept-source optical coherence tomography (SS-OCT) scan of the optic nerve head (ONH) of a glaucomatous eye. In the SS-OCT B-scan, from the reference line (white horizontal line) connecting both ends of the Bruch's membrane opening, three perpendicular lines were marked at the centre and $100 \mu\text{m}$ nasally and temporally. The anterior prelaminar depth (APLD, white vertical line) was defined as the distance from the reference line to the anterior prelaminar surface (grey horizontal dotted line). The prelaminar tissue thickness (PTT, black vertical dotted dash line) was defined as the distance from the anterior prelaminar surface to the anterior border of the lamina cribrosa (black horizontal dotted line). The representative value of the parameters for each patient was considered as the mean of three measurements obtained.

prelaminar surface. The prelaminar tissue thickness (PTT) was measured as the distance from the anterior prelaminar surface to the anterior border of the LC. For each patient, the representative value of a parameter was considered to be the mean of three measurements obtained by averaging the two graders' measurements. Figure 1 shows the landmarks used to measure the parameters.

Determination of glaucoma progression

Colour-disc photography, red-free RNFL photography and VF tests were performed and assessed according to each patient's regular 6-month follow-up visit. Progression of structural changes on disc and RNFL photography and functional changes on VF tests are as described below.

Structural change was determined by comparing serial stereo disc photography images of optic disc changes (i.e., focal or diffuse narrowing, neuroretinal rim notching, increased CDR, adjacent vasculature position shift). RNFL defect change by serial RNFL photography was defined as the appearance of a new defect or an increase in width or depth of an existing defect. Disc or RNFL changes were regarded as structural progression, and each patient was classified as a structural nonprogressor or progressor accordingly. Two observers (EB and YKK) masked to all patient information evaluated the photographs independently. In cases of disagreement, a third glaucoma specialist (KHP) served as an adjudicator.

Functional progression was evaluated by Guided Progression Analysis (GPA) software using the event-based algorithm of the Early Manifest Glaucoma Trial criteria

[22]. “Likely progression” was defined as 3 or more locations showing significant decreases in visual sensitivity (i.e., changes more than the test-retest variabilities) compared with 2 baseline examinations (separated by approximately 6 months in this study) for at least 3 consecutive tests, with decreases in visual sensitivity continuing to be detected in all subsequent follow-up visits. “Possible progression” was defined as three or more locations showing significant decreases in visual sensitivity compared with two baseline examinations for two consecutive tests, again with decreases in visual sensitivity continuing to be detected in all subsequent follow-up visits.

Statistical analyses

The Wilk–Shapiro test was used to determine the distribution of numerical data. The normally distributed data were compared by independent *t* test and the non-normally distributed data were compared by Mann–Whitney *U* test. The categorical data were analysed by chi-squared test. For validation of the agreement on LDS presence, ONH measurement, and determination of structural progression, the Kappa value and intra-class correlation coefficient (ICC), respectively, was calculated. Univariate logistic regression analysis was performed to evaluate the factors associated with LDS and glaucoma progression. Variables with a *P* value less than 0.10 in the univariate analysis were entered into the multivariate analysis. A backwards-elimination process was used to develop the final multivariate model. Data was presented as odds ratio (OR) with 95% confidence interval (CI). Statistical analyses were performed with the Statistical Package for Social Sciences version 21.0 for Windows (SPSS, Inc., Chicago, IL). A 2-sided *P* values < 0.05 were considered statistically significant.

Results

The study involved 84 POAG patients who had been followed up for 4.3 ± 1.2 years. The mean age was 58.9 ± 11.1 years (range 34 to 81), and 39 of the subjects were men (46.4%). The SE was -1.27 ± 2.30 D (-6.00 to 2.75); axial length, 23.76 ± 1.12 mm (21.76 to 26.29); baseline IOP, 14.3 ± 2.6 mmHg (10 to 19); mean IOP 12.8 ± 2.2 mmHg (10 to 19); MD, -2.16 ± 1.84 dB (-5.92 to 1.66). Based on SDPs, 53 subjects were classified as LDS and 31 as non-LDS. The demographic characteristics of the LDS group and non-LDS group are summarised in Table 1. Agreement on the presence of LDS and the determination of structural progression between the two graders was represented by a Kappa value of 0.778 ($P < 0.001$) and 0.772 ($P < 0.001$), respectively. The ICCs measured for confirmation of inter-examiner agreement were 0.991 for APLD and 0.981 for

PTT. There were no significant inter-group differences in demographic variables of age, sex, IOP, spherical equivalence, axial length, optic disc haemorrhage, parapapillary atrophy, follow-up period, and functional parameters.

Comparison of ONH structure between LDS and non-LDS glaucomatous eyes

Table 1 shows the ONH parameters measured by SS-OCT and SD-OCT. Eyes with LDS had significantly deeper APLD ($P < 0.001$) and thinner PTT ($P < 0.001$). In eyes with LDS, the APLD was 405.5 ± 107.6 μ m and the PTT was 74.3 ± 24.5 μ m; in eyes without LDS, the APLD was 302.5 ± 149.5 μ m and the PTT was 137.3 ± 40.1 μ m. In eyes with LDS, the average CDR, vertical CDR, rim area, disc area, and cup volume were 0.75 ± 0.06 , 0.76 ± 0.07 , 0.90 ± 0.19 mm², 2.17 ± 0.42 mm², and 0.52 ± 0.22 mm³, respectively, and in eyes without LDS, 0.58 ± 0.13 , 0.56 ± 0.17 , 1.08 ± 0.29 mm², 1.75 ± 0.38 mm², and 0.22 ± 0.15 mm³, respectively (all $P < 0.05$). The SS-OCT/SD-OCT parameters of RNFL thickness demonstrated no significant inter-group difference (Supplementary Table 1).

Possible factors associated with LDS in glaucoma

Table 2 and Supplementary Table 2 present the factors associated with LDS in glaucomatous eyes, as determined by univariate and multivariate logistic regression analyses. By multivariate analysis, only thin PTT was significantly associated with the LDS in glaucoma (OR = 0.939, $P = 0.001$) (Table 2). The other SD-OCT parameters showing significant association with LDS in the univariate analysis presented no such association in the multivariate analysis.

Structural and functional progression

The study eyes had a median number of 7 (range, 4–11) tests of SDP and RNFL photography and 7 (range 4–12) tests of the visual field during the follow-up period. Table 2 shows the results on progression. Significant progression was detected in the LDS group compared to non-LDS group (structural only, $P < 0.001$; functional only, $P = 0.025$, structural and functional, $P = 0.010$). In the LDS group of 53 patients, 45 (84.9 %) had structural progression, 23 (43.4 %) demonstrated VF progression (15.1% likely progression, 28.3% possible progression), and 22 (41.5 %) had both structural and functional glaucoma progression. In the non-LDS group of 31 patients, 8 (25.8 %) had structural progression, 6 (19.4 %) demonstrated VF progression (12.9% likely progression, 6.5% possible progression), and 5 (16.1 %) had both structural and functional glaucoma progression. The rate of VF progression was faster in the LDS group, but the difference was not statistically significant

Table 1 Comparison of demographic and clinical characteristics between patients with and without laminar dot sign.

	Total (n = 84)	LDS (n = 53)	Non-LDS (n = 31)	P value
Demographic variables				
Age (years)	58.9 ± 11.1	59.60 ± 11.39	57.65 ± 10.75	0.52*
Male, n (%)	39 (46.4)	22 (41.5)	17 (54.8)	0.24 [†]
Baseline intraocular pressure (mmHg)	14.3 ± 2.6	14.1 ± 2.6	14.6 ± 2.6	0.28*
Mean intraocular pressure (mmHg)	12.8 ± 2.2	12.7 ± 2.4	12.9 ± 2.1	0.66*
Spherical equivalence (D)	-1.27 ± 2.30	-1.00 ± 2.02	-1.80 ± 2.75	0.37*
Axial length (mm)	23.76 ± 1.12	23.66 ± 1.13	23.93 ± 1.13	0.49*
Optic disc haemorrhage, n (%)	22 (26.2)	13 (24.5)	9 (29.0)	0.65 [†]
Parapapillary atrophy, n (%)	73 (86.9)	47 (88.7)	26 (83.9)	0.08 [†]
Follow-up period (years)	4.34 ± 1.16	4.53 ± 1.17	4.00 ± 1.09	0.10*
SS-OCT (Deep ONH parameters)				
APLD (µm)	367.5 ± 133.5	405.5 ± 107.6	302.5 ± 149.5	<0.001[‡]
PTT (µm)	97.6 ± 43.5	74.3 ± 24.5	137.3 ± 40.1	<0.001[‡]
SD-OCT (2D-plane ONH parameters)				
Average CDR	0.69 ± 0.13	0.75 ± 0.06	0.58 ± 0.13	<0.001*
Vertical CDR	0.69 ± 0.15	0.76 ± 0.07	0.56 ± 0.17	<0.001*
Rim area (mm ²)	0.97 ± 0.24	0.90 ± 0.19	1.08 ± 0.29	0.002*
Disc area (mm ²)	2.02 ± 0.45	2.17 ± 0.42	1.75 ± 0.38	<0.001*
Cup volume (mm ³)	0.41 ± 0.25	0.52 ± 0.22	0.22 ± 0.15	<0.001*
Visual field parameters				
MD (dB)	-2.16 ± 1.84	-2.20 ± 1.84	-2.10 ± 1.86	0.86*
PSD (dB)	4.14 ± 2.48	3.97 ± 2.48	4.43 ± 2.50	0.37*
VFI (%)	94.31 ± 4.68	94.34 ± 4.73	94.26 ± 4.67	0.99*

Mean ± standard deviation.

Comparison between LDS and non-LDS group was performed by *independent *t*-test, [‡]Mann–Whitney *U* test, and [†]Chi-square test. Values with statistical significance are shown in bold.

LDS laminar dot sign; SS-OCT swept-source optical coherence tomography; SD-OCT spectral-domain optical coherence tomography; ALPD anterior prelaminar depth; PTT prelaminar tissue thickness; SD-OCT spectral-domain optical coherence tomography; CDR cup-to-disc ratio; MD mean deviation; dB decibels; PSD pattern standard deviation; VFI visual-field index.

($P = 0.15$). Chi-square test revealed that eyes with LDS had a significantly higher risk of glaucoma progression ($\chi^2 = 5.00$, degree of freedom = 1, $P = 0.033$).

Factors associated with glaucoma progression

The baseline factors were analysed by univariate and multivariate models. The factors associated with structural and functional progression are presented in Table 3. LDS and disc haemorrhage significantly contributed to glaucoma progression.

Representative cases

Figure 2 presents representative glaucoma cases with and without LDS followed for 5 years. The patient with LDS at the initial exam demonstrated structural and functional progression (Fig. 2a), while the patient without LDS presented a stable course (Fig. 2b).

Discussion

In the present study, we investigated the deep structure of the ONH as well as the LDS in glaucomatous eyes using both SD-OCT and SS-OCT and demonstrated the association with glaucoma progression. Eyes with LDS had thinner PTT, and, during a 4-year prospective follow-up period, they showed a significant association with structural and functional progression.

The LDS, first described by Read and Spaeth in 1974, is a morphologic sign observed under ophthalmoscope and on disc photography [17]. A previous clinical study on the LDS reported prevalences of 29.3% in normal eyes and 70.8% in open-angle glaucomatous eyes, the latter associated with larger vertical CDR and optic disc diameter [18]. Also in our study, glaucoma eyes with LDS had significantly larger CDR, thinner rim area, larger disc area, and larger cup volume compared with eyes without LDS. The difference can be expected to be due to the loss of neural

Table 2 Factors associated with laminar dot sign.

	Univariate				Multivariate			
	Beta	Wald	OR (95% CI)	P value	Beta	Wald	OR (95% CI)	P value
Demographic data								
Age (years)	0.016	0.608	1.016 (0.976–1.058)	0.44				
Male	0.537	1.387	1.711 (0.700–4.182)	0.24				
Baseline intraocular pressure (mmHg)	−0.078	0.75	0.925 (0.776–1.103)	0.38				
Mean intraocular pressure (mmHg)	−0.038	0.144	0.962 (0.789–1.173)	0.70				
Spherical equivalence (D)	0.152	1.608	1.164 (0.921–1.471)	0.21				
Axial length (mm)	−0.218	0.686	0.804 (0.480–1.347)	0.41				
Optic disc haemorrhage	−0.230	0.205	0.794 (0.293–2.152)	0.65				
Parapapillary atrophy	0.410	0.394	1.506 (0.419–5.417)	0.53				
Structural parameters								
APLD (μm)	0.007	10.247	1.007 (1.003–1.011)	0.001	−0.006	1.193	0.994 (0.984–1.005)	0.28
PTT (μm)	−0.074	20.915	0.929 (0.900–0.959)	<0.001	−0.063	10.266	0.939 (0.903–0.976)	0.001
Average CDR (0.01)	0.221	18.521	1.247 (1.128–1.379)	<0.001				
Vertical CDR (0.01)	0.176	19.434	1.193 (1.103–1.290)	<0.001	0.094	1.694	1.098 (0.954–1.265)	0.19
Rim area (mm ²) (0.1)	−0.333	8.456	0.717 (0.572–0.897)	0.004	−0.624	1.354	0.536 (0.187–1.533)	0.54
Disc area (mm ²) (0.1)	0.279	12.930	1.322 (1.135–1.539)	<0.001	0.269	1.668	1.309 (0.870–1.969)	0.20
Cup volume (mm ³) (0.1)	0.781	18.356	2.184 (1.528–3.122)	<0.001				
Functional parameters								
MD (dB)	−0.028	0.051	0.973 (0.763–1.240)	0.82				
PSD (dB)	−0.075	0.686	0.928 (0.777–1.108)	0.41				
VFI (%)	0.004	0.006	1.004 (0.913–1.104)	0.94				

Values with statistical significance are shown in bold.

OR odds ratio; CI confidence interval; D dioptres; ALPD anterior prelaminar depth; PTT prelaminar tissue thickness; CDR cup-to-disc ratio; MD mean deviation; dB decibels; PSD pattern standard deviation; VFI visual field index.

tissue and deep optic disc cupping in LDS eyes. We attempted to clarify the deep ONH structure of the LDS by recent image modalities of OCT providing high-resolution images. According to three-dimensional parameters of the SS-OCT, the LDS group had significantly deeper APLD and thinner PTT. In the univariate model, both APLD and PTT were associated with LDS; however, the analysis based on the multivariable model showed a relationship with only PTT. The other demographic findings, those on age, sex, IOP, axial length, disc haemorrhage, and parapapillary atrophy, as well as the functional parameters of the visual field, had no association with LDS. As expected, we could indicate that thin PTT is the main morphologic cause of LDS visibility, and that given its thin structure, we can observe the LDS under ophthalmoscopy and on SDP.

Many previous studies on PTT have reported the influence of high IOP on thin prelaminar thickness [6, 23, 24]. To minimise the high-pressure effect, therefore, from our ongoing prospective study of *SOS-LC*, patients with normal-range IOP (≤ 21 mmHg at baseline and during follow-up period) were enrolled. Baseline and follow-up mean IOP did not show any association with LDS or PTT. However, IOP-related strain is affected by the three-

dimensional ONH anatomy and features, which can vary among individuals and result, accordingly, in findings of non-associations of LC parameters with IOP [25]. Thus, even though the glaucoma patients included in the present study had a normal range of IOP, the effect of IOP should be interpreted with caution. Additionally, further studies with various values of IOP, including high ones, need to be conducted.

This study was based on early-glaucoma patients. A previous study on LC deformation found that deformation occurs mostly in the early stage of glaucoma [26]. Park et al. compared LC depth for different stages of glaucoma, and reported LD posterior displacement mostly in the early-glaucoma stage, but with no significant difference relative to the severe stage [27]. Kim et al. found no difference in LC deformity between mild and moderate-to-advanced glaucoma, also indicating that LC posterior bowing occurs in the early stage of glaucoma [19]. Jung et al. reported a difference in PTT between POAG and NTG, which discrepancy was greater in early glaucoma than in moderate or severe glaucoma [24].

In the present study, at the baseline exam, structural parameters (i.e., SD-OCT and SS-OCT parameters) differed

Table 3 Univariate and multivariate odds ratios and 95% confidence intervals of significant risk factors for each of structural and/or functional deterioration in patients with primary-open-angle glaucoma.

	Structural			Functional			Structural or functional		
	Beta	OR (95% CI)	P value	Beta	OR (95% CI)	P value	Beta	OR (95% CI)	P value
Univariate analysis									
Lamina dot sign	2.621	13.750 (4.668–40.500)	<0.001	1.465	4.327 (1.528–12.255)	0.006	2.777	3.063 (1.290–7.778)	<0.001
Disc haemorrhage	2.108	6.235 (1.770–8.307)	0.007	0.767	2.154 (0.745–6.231)	0.16	2.043	2.714 (1.657–5.905)	0.009
Rim area (mm ²)	–3.093	0.045 (0.005–0.404)	0.006	–0.336	0.715 (0.555–0.921)	0.009	0.024	1.024 (0.880–1.193)	0.76
Disc area (mm ²)	0.142	1.153 (1.025–1.297)	0.018	0.086	1.090 (0.982–1.209)	0.11	0.136	1.146 (1.039–1.263)	0.006
Multivariate analysis									
Lamina dot sign	4.238	6.299 (4.146–9.562)	<0.001	1.173	3.231 (1.115–9.358)	0.031	1.667	3.151 (1.488–4.868)	0.001
Disc haemorrhage	4.338	7.522 (4.342–9.332)	0.001				1.612	3.051 (1.658–4.688)	0.003

OR odds ratio; CI confidence interval.

significantly between eyes with and without LDS, while functional parameters (i.e., VF data) did not present any difference. Previous studies have reported a possible ‘structure-function dissociation’ (i.e., a discrepancy between structural and functional damage in glaucoma) [28], as well as the possibility that in glaucoma progression, structural damage and functional progression might not always occur sequentially [29–31]. This was also demonstrated in our study in terms of structural deterioration (by disc and/or RNFL photography) and functional deterioration (by GPA software). One functional progressor from each group of LDS and non-LDS, did not show definite structural change. While structural change can be indicative of subsequent functional damage, visual field defect might not always precede structural deterioration and attention on both sides are needed [29–31]. However, in the search for factors associated with glaucoma progression, the presence of LDS was significantly and prospectively associated with structural and functional progression. This finding suggests that LDS can add information to the assessment of disease progression risk.

The present study has limitations that include a relatively small sample size and a short follow-up period. Also, only patients with normal IOP values were included, and neither a normal population nor a moderate-to-severe glaucoma group from our ongoing prospective study of *SOS-LC* was included. Further studies based on a broader range of population groups are required. Moreover, although the presence of LDS was associated with functional progression, there was no difference in the rate between the LDS and non-LDS groups. The small sample size and possibility of different regions and VF test points might have affected the rate of progression. However, to our knowledge, this is the first study to compare OCT findings with and without LDS and their associations with glaucoma progression.

In conclusion, eyes with LDS had thinner PTT and deeper APLD as viewed under SS-OCT and were significantly associated with risk of glaucoma progression. Knowledge of the ONH’s deep structure and the LDS and their relationship with glaucoma progression may provide information relevant to close inspection of the ONH of LDS patients.

Summary

What was known before

- The lamina dot sign is one classical optic nerve head sign of glaucoma in inspections of the lamina cribrosa area. It is the visible grey pores or fenestrae that develop by the loss of neural tissue and deep optic disc cupping, exposing the underlying lamina cribrosa tissue.

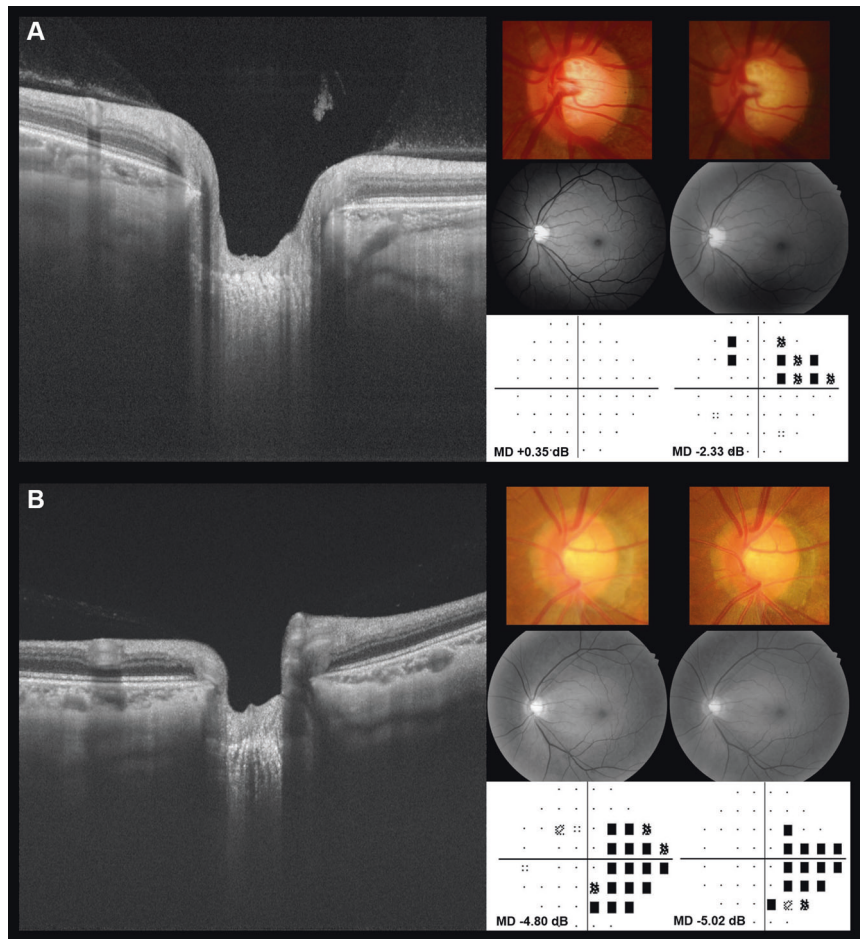


Fig. 2 Representative cases with and without laminar dot sign. a Left eye of a 44-year-old open-angle glaucoma female demonstrated progressive structural and functional change during a 5 year follow-up. At the initial exam, her baseline intraocular pressure (IOP) was 16 mmHg, the spherical equivalence (SE) was -5.13 D, and the mean deviation (MD) was $+0.35$ dB. (left) Measurement of optic nerve head (ONH) structure by swept-source optical coherence tomography (SS-OCT)-acquired image presented anterior prelaminar depth of 422 μm and prelaminar tissue thickness of 72 μm . (right, top) Progressive inferior disc rim narrowing (right, middle) with corresponding inferior retinal nerve fibre layer (RNFL) defect widening. (right, bottom) and

progressive visual field defect in the pattern deviation plot (MD of -2.33 dB) was observed. **b** Left eye of a 47-year-old female demonstrated no progressive structural or functional change during 5-year follow-up. At the initial exam, her baseline IOP was 15 mmHg, the SE was -5.25 D, and the MD was -4.80 dB. (left) In the SS-OCT-acquired image of the ONH structure, anterior prelaminar depth was 198 μm and prelaminar tissue thickness was 153 μm . (right, top) Inferior rim narrowing on disc photography, (right, middle), corresponding inferior RNFL defect on RNFL photography and (right, bottom) visual field defect in pattern deviation plot (MD of -5.02 dB) appeared stable.

What this study adds

- This study evaluated the deep optic nerve head of eyes with and without laminar dot sign by using optical coherence tomography, and demonstrated the prospective association with glaucoma progression.

Compliance with ethical standards

Conflict of interest The authors declare that they have no conflict of interest.

Publisher's note Springer Nature remains neutral with regard to jurisdictional claims in published maps and institutional affiliations.

References

1. Hernandez MR, Igoe F, Neufeld AH. Extracellular matrix of the human optic nerve head. *Am J Ophthalmol.* 1986;102:139–48.
2. Anderson DR, Hoyt WF. Ultrastructure of intraorbital portion of human and monkey optic nerve. *Arch Ophthalmol.* 1969;82: 506–30.
3. Lee EJ, Kim TW, Kim M, Kim H. Influence of lamina cribrosa thickness and depth on the rate of progressive retinal nerve fiber layer thinning. *Ophthalmology.* 2015;122:721–9.
4. Kim DW, Jeoung JW, Kim YW, Girard MJ, Mari JM, Kim YK, et al. Prelamina and lamina cribrosa in glaucoma patients with unilateral visual field loss. *Investig Ophthalmol Vis Sci.* 2016;57:1662–70.
5. Parrish RK 2nd, Feuer WJ, Schiffman JC, Lichter PR, Musch DC. Five-year follow-up optic disc findings of the Collaborative Initial

- Glaucoma Treatment Study. *Am J Ophthalmol.* 2009;147:717–24. e1
6. Reis AS, O'Leary N, Stanfield MJ, Shuba LM, Nicoleta MT, Chauhan BC. Lamellar displacement and prelaminar tissue thickness change after glaucoma surgery imaged with optical coherence tomography. *Invest Ophthalmol Vis Sci.* 2012;53:5819–26.
 7. Barrancos C, Rebolleda G, Oblanca N, Cabarga C, Munoz-Negrete FJ. Changes in lamina cribrosa and prelaminar tissue after deep sclerectomy. *Eye.* 2014;28:58–65.
 8. Agoumi Y, Sharpe GP, Hutchison DM, Nicoleta MT, Artes PH, Chauhan BC. Lamellar and prelaminar tissue displacement during intraocular pressure elevation in glaucoma patients and healthy controls. *Ophthalmology.* 2011;118:52–9.
 9. Trivli A, Koliarakis I, Terzidou C, Goulielmos GN, Siganos CS, Spandidos DA, et al. Normal-tension glaucoma: pathogenesis and genetics. *Exp Ther Med.* 2019;17:563–74.
 10. Mozaffarieh M, Flammer J. New insights in the pathogenesis and treatment of normal tension glaucoma. *Curr Opin Pharmacol.* 2013;13:43–49.
 11. Huang D, Swanson EA, Lin CP, Schuman JS, Stinson WG, Chang W, et al. Optical coherence tomography. *Science.* 1991;254:1178–81.
 12. Schuman JS, Pedut-Kloizman T, Pakter H, Wang N, Guedes V, Huang L, et al. Optical coherence tomography and histologic measurements of nerve fiber layer thickness in normal and glaucomatous monkey eyes. *Investig Ophthalmol Vis Sci.* 2007;48:3645–54.
 13. Spaide RF, Koizumi H, Pozzoni MC. Enhanced depth imaging spectral-domain optical coherence tomography. *Am J Ophthalmol.* 2008;146:496–500.
 14. Srinivasan VJ, Adler DC, Chen Y, Gorczynska I, Huber R, Duker JS, et al. Ultrahigh-speed optical coherence tomography for three-dimensional and en face imaging of the retina and optic nerve head. *Invest Ophthalmol Vis Sci.* 2008;49:5103–10.
 15. Deleon-Ortega JE, Arthur SN, McGwin G Jr., Xie A, Monheit BE, Girkin CA. Discrimination between glaucomatous and non-glaucomatous eyes using quantitative imaging devices and subjective optic nerve head assessment. *Investig Ophthalmol Vis Sci.* 2006;47:3374–80.
 16. Vessani RM, Moritz R, Batis L, Zagui RB, Bernardoni S, Susanna R. Comparison of quantitative imaging devices and subjective optic nerve head assessment by general ophthalmologists to differentiate normal from glaucomatous eyes. *J Glaucoma.* 2009;18:253–61.
 17. Read RM, Spaeth GL. The practical clinical appraisal of the optic disc in glaucoma: the natural history of cup progression and some specific disc-field correlations. *Trans Am Acad Ophthalmol Otolaryngol.* 1974;78:Op255–74.
 18. Healey PR, Mitchell P. Visibility of lamina cribrosa pores and open-angle glaucoma. *Am J Ophthalmol.* 2004;138:871–2.
 19. Kim YW, Jeoung JW, Kim DW, Girard MJ, Mari JM, Park KH, et al. Clinical assessment of lamina cribrosa curvature in eyes with primary open-angle glaucoma. *PLoS ONE.* 2016;11:e0150260.
 20. Girard MJ, Tun TA, Husain R, Acharyya S, Haaland BA, Wei X, et al. Lamina cribrosa visibility using optical coherence tomography: comparison of devices and effects of image enhancement techniques. *Investig Ophthalmol Vis Sci.* 2015;56:865–74.
 21. Mari JM, Strouthidis NG, Park SC, Girard MJ. Enhancement of lamina cribrosa visibility in optical coherence tomography images using adaptive compensation. *Investig Ophthalmol Vis Sci.* 2013;54:2238–47.
 22. Heijl A, Leske MC, Bengtsson B, Bengtsson B, Hussein M. Measuring visual field progression in the Early Manifest Glaucoma Trial. *Acta Ophthalmol Scand.* 2003;81:286–93.
 23. Lee EJ, Kim TW, Weinreb RN. Reversal of lamina cribrosa displacement and thickness after trabeculectomy in glaucoma. *Ophthalmology.* 2012;119:1359–66.
 24. Jung YH, Park HY, Jung KI, Park CK. Comparison of prelaminar thickness between primary open angle glaucoma and normal tension glaucoma patients. *PLoS ONE.* 2015;10:e0120634.
 25. Burgoyne CF, Downs JC, Bellezza AJ, Suh JK, Hart RT. The optic nerve head as a biomechanical structure: a new paradigm for understanding the role of IOP-related stress and strain in the pathophysiology of glaucomatous optic nerve head damage. *Prog Retin Eye Res.* 2005;24:39–73.
 26. Bellezza AJ, Rintalan CJ, Thompson HW, Downs JC, Hart RT, Burgoyne CF. Deformation of the lamina cribrosa and anterior scleral canal wall in early experimental glaucoma. *Investig Ophthalmol Vis Sci.* 2003;44:623–37.
 27. Park SC, Brumm J, Furlanetto RL, Netto C, Liu Y, Tello C, et al. Lamina cribrosa depth in different stages of glaucoma. *Investig Ophthalmol Vis Sci.* 2015;56:2059–64.
 28. Malik R, Swanson WH, Garway-Heath DF. 'Structure-function relationship' in glaucoma: past thinking and current concepts. *Clin Exp Ophthalmol.* 2012;40:369–80.
 29. Kass MA, Heuer DK, Higginbotham EJ, Johnson CA, Keltner JL, Miller JP, et al. The Ocular Hypertension Treatment Study: a randomized trial determines that topical ocular hypotensive medication delays or prevents the onset of primary open-angle glaucoma. *Arch Ophthalmol.* 2002;120:701–13. discussion 829–30
 30. Medeiros FA, Alencar LM, Zangwill LM, Bowd C, Sample PA, Weinreb RN. Prediction of functional loss in glaucoma from progressive optic disc damage. *Arch Ophthalmol.* 2009;127:1250–6.
 31. Chauhan BC, Nicoleta MT, Artes PH. Incidence and rates of visual field progression after longitudinally measured optic disc change in glaucoma. *Ophthalmology.* 2009;116:2110–8.